Expanded View Figures

Figure EV1. Rheb mediates mitophagy initiation in axons that requires Nix.

A, B   Representative kymographs (A) and quantitative analysis (B) showing that $\Delta\psi_m$ depolarization increases retrograde transport but reduces anterograde transport of mitochondria along axons. The relative motility of mitochondria in axons treated with DMSO or CCCP was quantified (B). Data were quantified from the total number of neurons (*n*) indicated in parentheses (B) from more than four experiments.

C, D   Quantitative analysis (C) and representative kymographs (D) showing robust recruitment of Rheb to depolarized mitochondria within axons after treatment with antimycin A (AA). The percentage of white arrow-indicated mitochondria that were targeted by Rheb in the presence or absence of AA was quantified (C).

E   Representative triple-channel images showing that Rheb-associated mitochondria are targeted to autophagy after CCCP treatment. Rheb-tagged mitochondria (marked by arrows) are positive for LC3, whereas LC3 cannot be detected on mitochondria without Rheb association.

F   Rab7, a late endosome/amphisome marker, is associated with Rheb-targeted mitophagosomes as indicated by white arrows within axons under CCCP treatment.

G, H   Representative images (G) and quantitative analysis (H) showing that Nix RNAi reduces mitochondrial recruitment of Rheb in axons upon CCCP-induced $\Delta\psi_m$ dissipation. The percentage of mitochondria targeted by Rheb (white arrows) in axons expressing scrambled shRNA or Nix shRNA was quantified (H).

I, J   Impaired biogenesis of mitophagosomes within CCCP-treated axons expressing Nix shRNA. Note that Rheb-associated mitophagosomes are markedly decreased following Nix RNAi. The number of Rheb-targeted autophagic vacuoles (AVs) (Rheb-AVs) labeled by white arrows in axons expressing scrambled shRNA or Nix shRNA was quantified (J).

Data information: Data were quantified from the total number of neurons (*n*) indicated in parentheses (B) or on the top of the bars (C, H, J) from at least four experiments. Scale bars: 10 μm. Error bars represent SEM. Student's *t*-test: ***P < 0.001.
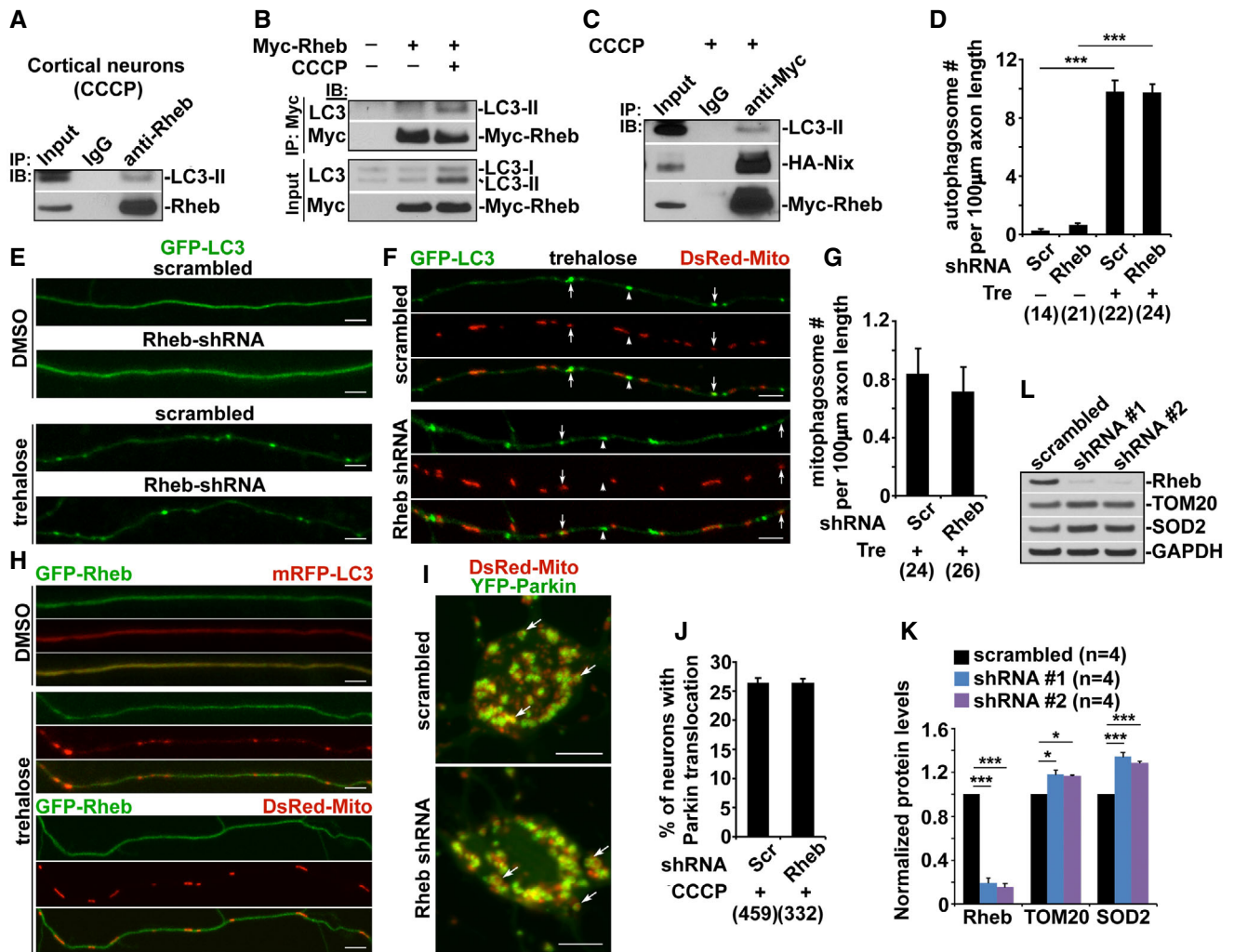
Figure EV2. Rheb is involved in mitophagy but not autophagy in axons.

A   Rheb-LC3-II complex was immunoprecipitated by the antibody against Rheb, but not normal IgG control, from the lysates of cortical neurons treated with CCCP.

B   Rheb-LC3-II complex was detected in the lysates of transfected HeLa cells treated with CCCP, but not DMSO control.

C   Immunoprecipitation of Myc-Rheb with LC3-II and HA-Nix from HeLa cell lysates with an anti-Myc antibody or normal IgG as a control in the presence of CCCP.

D–G   Representative images (E, F) and quantitative analysis (D, G) showing that Rheb RNAi has no detectable effects on trehalose (Tre)-induced autophagy in axons. The numbers of axonal autophagosomes (E) and mitophagosomes (white arrows in F) in neurons expressing scrambled shRNA or Rheb shRNA were quantified in the presence of DMSO or trehalose, respectively (D, G).

H   Rheb is enriched in cytoplasm under basal conditions and is not associated with either autophagosomes or mitochondria in axons upon trehalose treatment.

I, J   Representative images (I) and quantitative analysis (J) showing that Rheb is not required for Parkin-dependent mitophagy in the soma upon Δψ$_m$ dissipation. The percentage of total neurons displaying Parkin localization to mitochondria indicated by white arrows in the soma of CCCP-treated neurons expressing scrambled shRNA or Rheb shRNA was quantified (J).

K, L   Quantitative analysis (K) and representative blots (L) showing knockdown efficiency of Rheb shRNA (small hairpin RNA, (shRNA) #1 and shRNA #2), and silencing effects on mitochondrial degradation respective to control (scrambled shRNA) in HEK293 cells. Data were quantified from four independent repeats.

Data information: Data were quantified from the total number of neurons (*n*) indicated in parentheses (D, G, J) from at least four independent experiments. Scale bars: 10 μm. Error bars represent SEM. Student's *t*-test: ***$P < 0.001$; *$P < 0.05$.
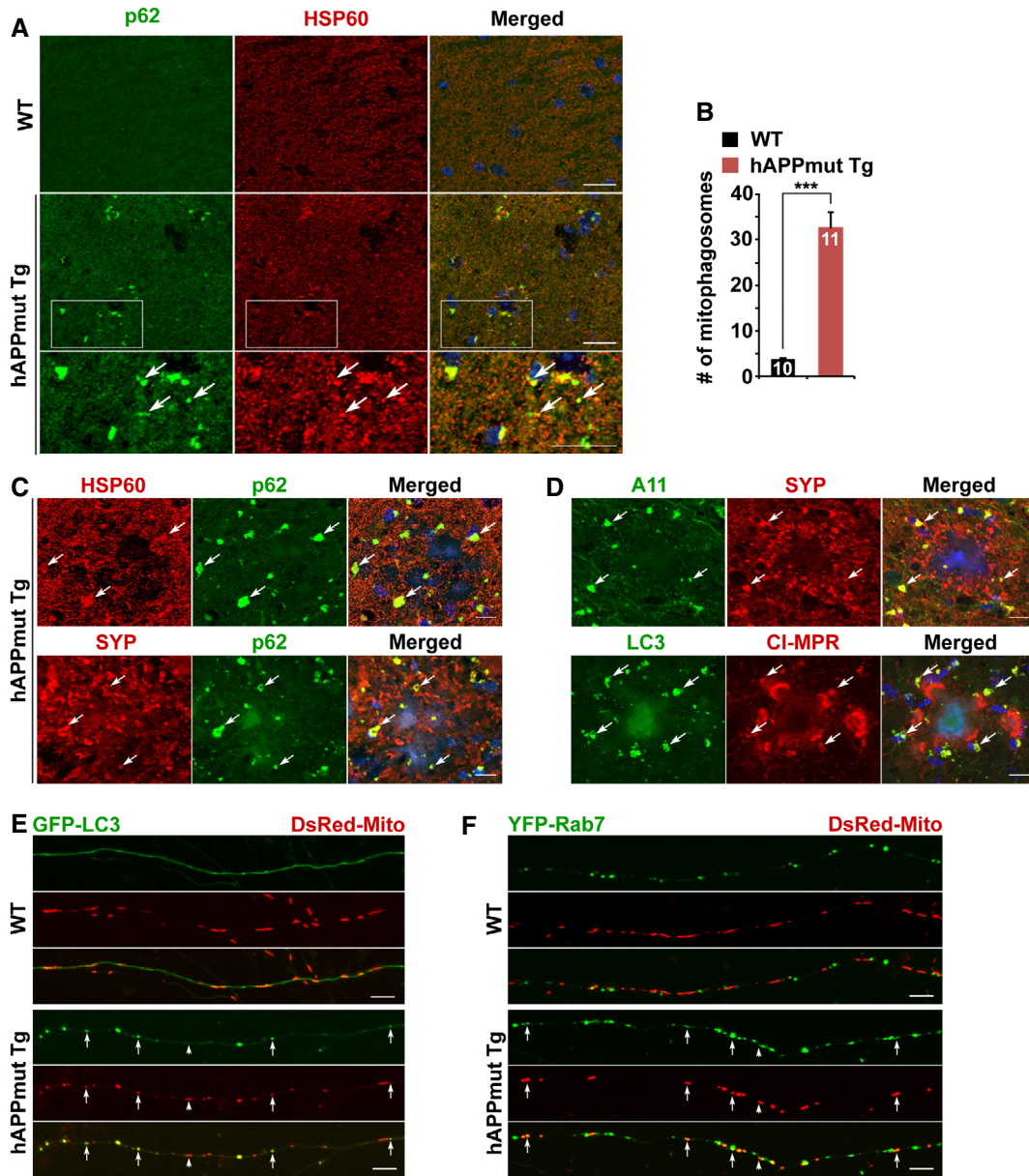
Figure EV3. Mitophagy stress in the axons and within the dystrophic presynaptic terminals of AD-related mutant hAPP neurons.

A, B   Representative images (A) and quantitative analysis (B) showing aberrant accumulation of mitophagosomes co-labeled by antibodies against p62 and HSP60 in the hippocampal mossy fibers of mutant hAPP Tg mouse brains. Note that mitophagosomes labeled by white arrows are not readily observed in WT mouse brains. The average number of mitophagosomes per section (320 μm × 320 μm) was quantified from the total number of brain slice sections (n) indicated on the top of the bars (B).

C, D   Representative images showing that mitophagosomes labeled by antibodies against p62 and HSP60 are concentrated within dystrophic presynaptic terminals indicated by synaptophysin (SYP). Note that soluble oligomeric Aβ marked by A11 antibody is enriched within swollen axonal terminals surrounding amyloid plaques in the hippocampal regions of mutant hAPP Tg mouse brains. Accumulated mitophagosomes (white arrows) are mito-amphisomes in nature that are positive for cation-independent mannose 6-phosphate receptor (CI-MPR), a late endosome (LE) marker.

E   Abnormal accumulation of mitophagosomes within the axons of mutant hAPP Tg neurons. Note that a significant portion of mitochondria in mutant hAPP axons are retained within LC3-marked autophagic vacuoles (AVs). Mitophagosomes indicated by white arrows are not readily detected within WT axons.

F   Mitochondria were trapped within Rab7-labeled amphisomes as mito-amphisomes (white arrows) within mutant hAPP Tg axons.

Data information: Scale bars: 25 μm (A) and 10 μm (C–F). Error bars represent SEM. Student's t-test: ***P < 0.001.
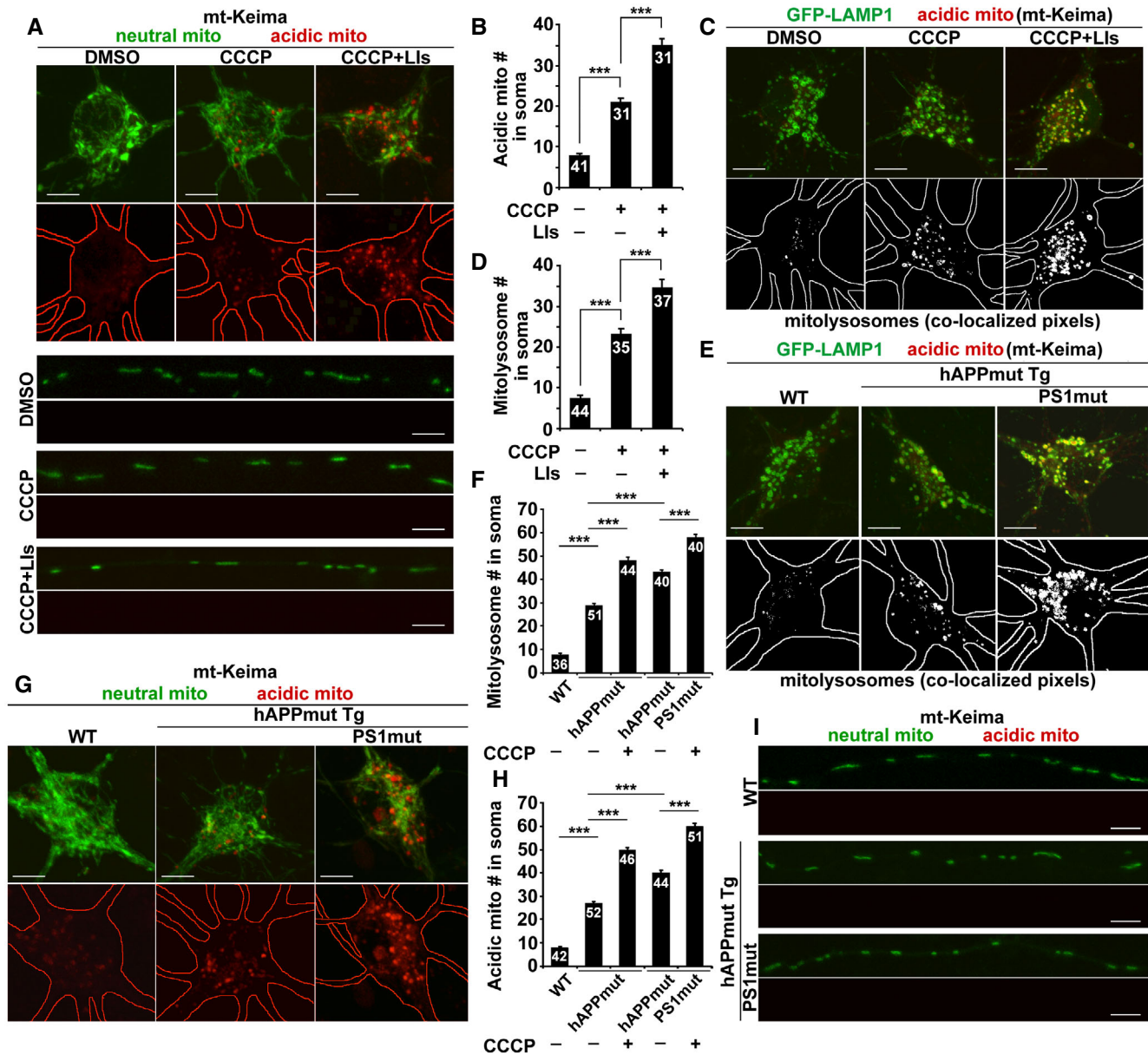
Figure EV4. Lysosomal impact on mitophagy in the soma but not in the axons of AD neurons.

A, B   Representative images (A) and quantitative analysis (B) showing that acidic mitochondria are present in the soma but not in the axons of neurons. Cortical neurons were transfected with mt-Keima, followed by treatment with DMSO, CCCP, or CCCP and lysosomal inhibitors (LIs) prior to live-cell imaging. mt-Keima is a ratiometric pH-sensitive fluorescent probe that targets to the mitochondrial matrix. A short wavelength (440 nm) is predominant for excitation in a neutral environment (neutral mito), whereas a long wavelength (586 nm) is predominant in an acidic environment (acidic mito). Note increased numbers of acidic mitochondria in the soma treated with CCCP or CCCP and LIs, but not in axons under these conditions. The number of acidic mitochondria (mito) in the soma of neurons was quantified (B).

C, D   Imaging of mt-Keima and GFP-LAMP1 shows that acidic mitochondria are mostly retained within LAMP1-marked lysosomes in the soma (C). The number of mitolysosomes co-labeled by LAMP1 and mt-Keima was quantified in the soma of neurons treated with DMSO, CCCP, or CCCP with LIs (D).

E, F   Representative images (E) and quantitative analysis (F) showing aberrant accumulation of mitolysosomes in the soma. The number of mitolysosomes was quantified in the soma of WT neurons, mutant hAPP neurons, or mutant hAPP neurons expressing mutant PS1 with or without CCCP treatment (F). Note that aberrant accumulation of mitolysosomes is enhanced in AD neurons co-expressing mutant hAPP and mutant PS1 in the presence or absence of CCCP.

G–I   The presence of acidic mitochondria in the soma but not in the axons of AD neurons expressing mutant hAPP or mutant hAPP with mutant PS1. The number of acidic mitochondria in the soma of AD neurons was quantified in the presence or absence of CCCP (H).

Data information: Data were quantified from the total number of neurons (*n*) indicated on the top of the bars from at least four experiments. Scale bars: 10 μm. Error bars represent SEM. Student's *t*-test: ***P < 0.001.
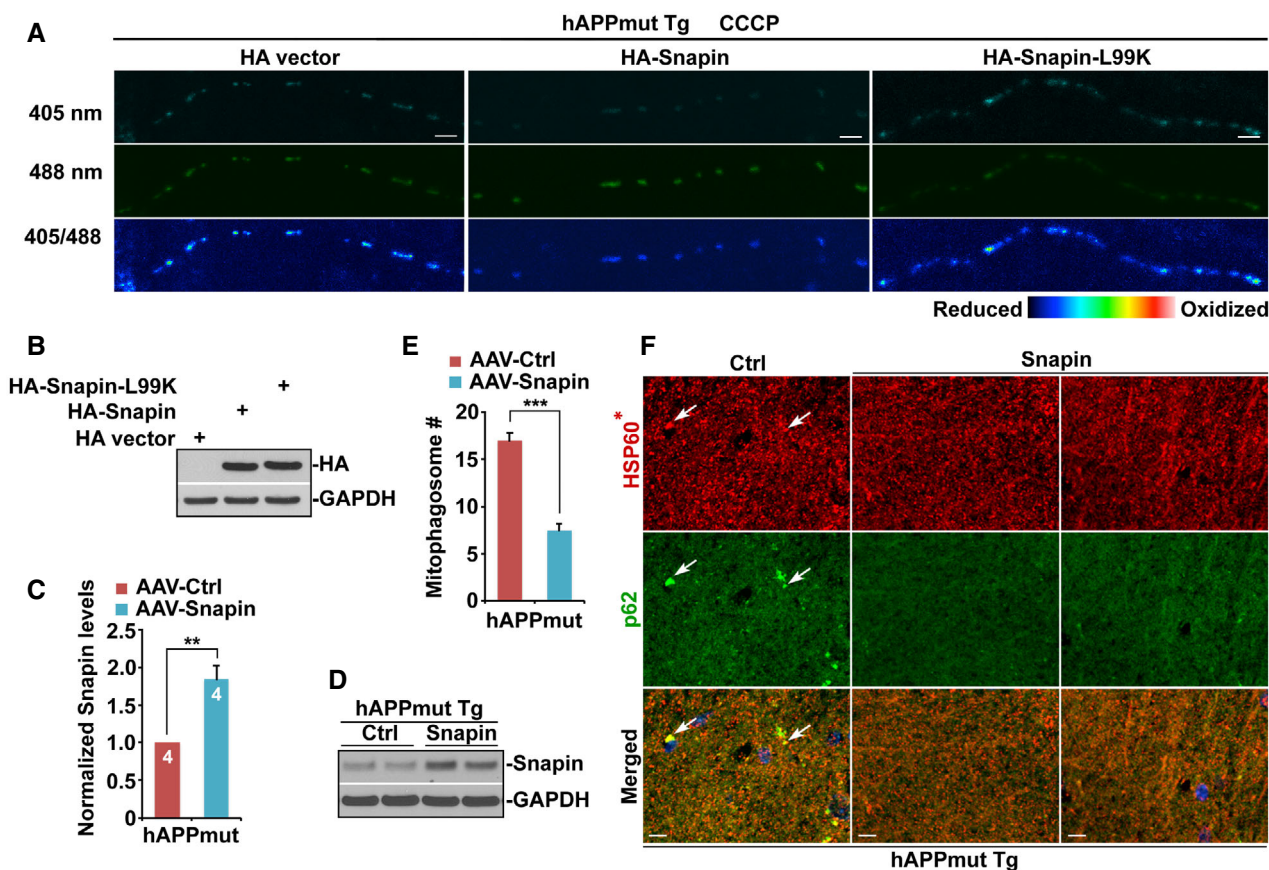
Figure EV5. Overexpression of Snapin reduces mitochondrial stress in the axons of mutant hAPP neurons.

A   Representative images showing oxidatively stressed mitochondria within mutant hAPP axons expressing Snapin, Snapin-L99K, or vector control after CCCP treatment.

B   The expression levels of Snapin and Snapin-L99K in HEK293 cells. GAPDH is a loading control.

C, D   Quantitative analysis (C) and representative blots (D) showing elevated Snapin expression in the hippocampus of mutant hAPP Tg mouse brains after AAV injection. A total of 10 μg of hippocampal homogenates from mutant hAPP mice transduced with AAV-mCherry or AAV-mCherry-Snapin were sequentially immunoblotted on the same membrane after stripping between each antibody application. Relative protein levels were normalized by GAPDH and to that of control mutant hAPP mice injected with AAV-mCherry. Data were analyzed from four pairs of mice.

E, F   Quantitative analysis (E) and representative images (F) showing reduced mitophagic accumulation in the hippocampal mossy fiber regions of AD mice transduced with AAV-mCherry-Snapin. Note a significant reduction of white arrow-marked mitophagosomes that were co-labeled by HSP60 and p62 in mutant hAPP Tg mouse brains with overexpression of Snapin. HSP60*: Color is converted to red for better contrast (F). Data were quantified from a total number of 15–20 imaging slice sections of three pairs of mutant hAPP Tg mice with AAV injection.

Data information: Scale bars: 10 μm. Error bars represent SEM. Student's *t*-test: ***$P < 0.001$; **$P < 0.01$.